An Experimental and Analytical Study of High-Energy-Density Propellants for Liquid Rocket Engines

Timothy Kokan[*], John R. Olds[†]

Space Systems Design Lab
Guggenheim School of Aerospace Engineering
Georgia Institute of Technology, Atlanta, GA, 30332-0150
timothy_kokan@ae.gatech.edu

There exists wide ranging research interest in high-energy-density matter (HEDM) propellants as a potential replacement of existing industry standard fuels (LH2, RP-1, MMH, UDMH) for liquid rocket engines. The U.S. Air Force Research Laboratory[1,2], the U.S. Army Research Lab[3,4], and the NASA Marshall Space Flight Center[5] each have ongoing programs in the synthesis and development of these potential new propellants.

The thermophysical understanding of HEDM propellants is necessary to model their performance in the conceptual design of liquid rocket engines. Most industry standard powerhead design tools (e.g. NPSS, ROCETS, and REDTOP-2) require several thermophysical properties of a given propellant over a wide range of temperature and pressure. These properties include enthalpy, entropy, density, internal energy, specific heat, viscosity, and thermal conductivity. For most of these potential new HEDM propellants, this thermophysical data either does not exist or is incomplete over the range of temperature and pressure necessary for liquid rocket engine design and analysis.

The work presented is a technique for obtaining enthalpy and density data for new propellants through the use of a combination of analytical/computational methods (quantum mechanics[6] and molecular dynamics[7]) and experimental investigations. Details of this technique and its application to an example HEDM fuel currently of interest are provided.

Nomenclature

CER	=	cost estimating relationship
COMPASS	=	Condensed-phase Optimized Molecular Potentials for Atomistic Simulation Studies
DMAZ	=	2-azido-N, N-dimethylethanamine, $C_4H_{10}N_4$
HEDM	=	high-energy-density matter
I_{sp}	=	specific impulse (sec)
k_B	=	Boltzmann Constant ($1.38066*10^{-23}$ J/K)
NPSS	=	Numerical Propulsion System Simulation
REDTOP	=	Rocket Engine Design Tool for Optimal Performance
REDTOP-2	=	Rocket Engine Design Tool for Optimal Performance Release 2
ROCETS	=	Rocket Engine Transient Simulation
SSDL	=	Space Systems Design Lab
TFU	=	theoretical first unit
ZPE	=	zero-point energy

[*] Graduate Research Assistant, School of Aerospace Engineering, Student member AIAA.
[†] Associate Professor, School of Aerospace Engineering, Associate Fellow AIAA.

I.   Introduction

The scope of the research described here is to develop a technique for determining the thermophysical properties of potential new rocket engine propellants. The thermophysical understanding of rocket propellants is necessary to model their performance in the conceptual design of liquid rocket engines. Most industry standard powerhead design tools (e.g. NPSS, ROCETS, and REDTOP-2) require several thermophysical properties of a given propellant over a wide range of temperature and pressure. These properties include enthalpy, entropy, internal energy, specific heat, density, viscosity, and thermal conductivity. For most of these potential new propellants, this thermophysical data either does not exist or is incomplete over the range of temperature and pressure necessary for liquid rocket engine design and analysis. The research work presented focuses on two of these thermophysical properties: enthalpy and density. Work is ongoing to incorporate the prediction of entropy, viscosity, and thermal conductivity to fully describe all the needed thermophysical properties for conceptual powerhead design.

The technique used in this research work to determine enthalpy and density utilizes a combination of analytical/computational methods and experimental investigations. Quantum mechanical methods are used to model a single molecule of the desired propellant in isolation to determine its zero-point energy. The zero-point energy (ZPE) of a molecule is the energy that molecule would theoretically have if it were at a temperature of absolute zero. A design-of-experiments is performed with this molecule to determine the predicted ZPE over a range of geometries around the baseline molecular geometry. In this way, one can model the change in ZPE of the molecule as bond lengths, bond angles, and torsion angles are changed. This sensitivity in molecular ZPE as a function of the molecular geometry is useful in modeling a group of molecules together. The interaction of these molecules, their collisions with one another and resulting changes in velocity, can be used to measure all the necessary thermophysical properties. This technique of modeling a set of molecules and their collisions is known as molecular dynamics.

Once molecular dynamics simulations are run over a range of temperatures and pressures, the resulting calculated thermophysical properties can be imported into any of the aforementioned powerhead design tools. One can then perform conceptual rocket engine design with these new propellants. The end goal is to be able to incorporate new propellants into vehicle designs and quantify the benefits of these new propellants to the overall vehicle system and design architecture.

II.   Analysis Technique

Many thermophysical property prediction tools have been created for a variety of uses. Techniques ranging from new equations of state to quantum mechanics have been used to measure certain thermodynamic and physical properties. A recent method developed by Sun[8] utilizes molecular dynamics simulations to calculate many thermophysical properties of a variety of molecules. Sun developed a new molecular force-field called the COMPASS force field, which stands for Condensed-phase Optimized Molecular Potentials for Atomistic Simulation Studies. In molecular dynamics, these force-fields are energy potential fields of an atom or molecule that are used to model the effects of one particle on a neighboring particle. They model the bond, angle, and torsion energies within a molecule as well as the electrostatic and van der Waals energies between molecules.

The COMPASS force field parameters for the intramolecular terms are derived from curve fits of quantum mechanical data. The intermolecular force field parameters are determined by running molecular dynamics simulations and fitting the simulated thermophysical results to experimental data by adjusting the intermolecular parameters.

The COMPASS force field is shown in equation (1). The functions in the COMPASS model can be divided into two general categories: the first is the valence terms which represent the internal coordinates of the atoms that make up the molecule, and the second is the nonbond interaction terms which represent those interactions between atoms separated by two or more atoms or those that belong to different molecules[8]. The first ten terms in the equation belong to the first category while the last two terms belong to the second category. The first four terms represent bond lengths (b), bond angles (θ), torsion angles (ϕ), and out-of-plane angles (χ). The internal motions are shown in Figure 1. The next six terms are cross-coupling terms of two or more of the internal coordinates.

$$E_{pot}^{COMPASS} = \sum_b \left[k_2 (b - b_0)^2 + k_3 (b - b_0)^3 + k_4 (b - b_0)^4 \right]$$

$$+ \sum_\theta \left[h_2 (\theta - \theta_0)^2 + h_3 (\theta - \theta_0)^3 + h_4 (\theta - \theta_0)^4 \right]$$

$$+ \sum_\phi \left[V_1 (1 - \cos\phi) + V_2 (1 - \cos 2\phi) + V_3 (1 - \cos 3\phi) \right]$$

$$+ \sum_\chi K_\chi (\chi - \chi_0)^2$$

$$+ \sum_{b,b'} K_{bb'} (b - b_0)(b' - b_0')$$

$$+ \sum_{\theta,\theta'} K_{\theta\theta'} (\theta - \theta_0)(\theta' - \theta_0')$$

$$+ \sum_{b,\theta} K_{b\theta} (b - b_0)(\theta - \theta_0) \qquad (1)$$

$$+ \sum_{b,\phi} (b - b_0)\left[G_1 \cos\phi + G_2 \cos 2\phi + G_3 \cos 3\phi \right]$$

$$+ \sum_{\theta,\phi} (\theta - \theta_0)\left[F_1 \cos\phi + F_2 \cos 2\phi + F_3 \cos 3\phi \right]$$

$$+ \sum_{\theta,\theta',\phi} K_{\theta\theta'\phi} (\theta - \theta_0)(\theta' - \theta_0')(\phi - \phi_0)$$

$$+ \sum_{i,j} \frac{q_i q_j}{r_{ij}}$$

$$+ \sum_{i,j} \varepsilon_{ij} \left[2 \left(\frac{r_{ij}^0}{r_{ij}} \right)^9 - 3 \left(\frac{r_{ij}^0}{r_{ij}} \right)^6 \right]$$
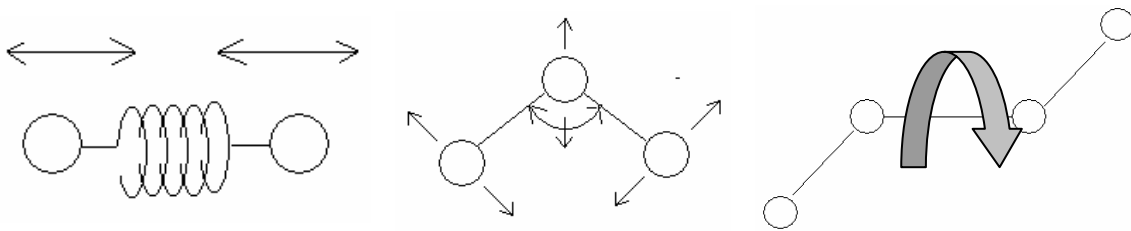

Figure 1. Bond Length, Bond Angle, and Torsion Angle Internal Motions

A. Quantum Mechanics

As shown in equation (1), several coefficients (k_i, h_i, V_i, K_i, etc.) are needed to define the energy potential. The coefficients for the first ten terms in equation (1) are derived from curve fits of quantum mechanical data. Sun[8] in 1998 and McQuaid[9] in 2004 did this work for several different atom types.

In the field of molecular design and energy prediction, quantum mechanical techniques attempt to either solve directly or approximate numerically the *wave function* of a system. The *wave function* describes the location of all the particles in the system as a function of time. In 1926, Austrian physicist Erwin Schrödinger developed an

equation for the wave function of a one-particle, one-dimensional system[6]. This equation, known as the time-dependent Schrödinger equation or Schrödinger wave equation is shown in equation (2).

$$-\frac{h}{2\pi i}\frac{\partial \Psi(x,t)}{\partial t} = -\frac{h^2}{8\pi^2 m}\frac{\partial^2 \Psi(x,t)}{\partial x^2} + V(x,t)\Psi(x,t) \tag{2}$$

In the above equation, Ψ is the time-dependent wave function, V is the potential energy function, h is Planck's constant, m is the mass of the particle, and i is the imaginary unit. As shown in equation (2), Schrödinger's wave equation contains the first derivative of the wave function. As a result, if one knows the wave function at any point in time, the wave function can be calculated for all future points in time. A variety of techniques are used to either solve this equation numerically for a given molecule or to approximate it[6].

Sun and McQuaid were able to make use of these techniques to compute the ZPE of a range of molecules at different atomic configurations perturbed from each molecule's respective minimum energy configuration. By doing this, one can obtain the energy surface of the molecule near the minimum energy configuration as a function of atom location. This energy surface can then be curve-fit with the COMPASS intramolecular terms by adjusting the aforementioned coefficients in equation (1).

B. Molecular Dynamics

Molecular dynamics is used initially to determine the appropriate values for the coefficients used in the intermolecular terms of the COMPASS potential model. These terms describe the intermolecular potential or potential between two atoms in different molecules or two atoms in the same molecule not connected through a bond, angle, or torsion.

Molecular dynamics is used in conjunction with experimental methods to determine these coefficient values. Molecular dynamics is a technique for modeling the motion and positions of particles subject to the laws of classical mechanics[10]. This approximation of the motion of particles that are actually governed by the laws of quantum mechanics may seem too overly simplified to produce accurate results, but is actually a very good approximation for a wide range of molecules[10].

The intermolecular potential parameters are initially set using a 6th order combination law for unlike atom pairs shown in equations (3) and (4). Parameter values for like atom pairs are known and thus those for unlike atom pairs can be computed very quickly.

$$r_{ij}^0 = \left[\frac{\left(r_i^0\right)^6 + \left(r_j^0\right)^6}{2}\right]^{1/6} \tag{3}$$

$$\varepsilon_{ij} = 2\sqrt{\varepsilon_i \varepsilon_j}\left[\frac{\left(r_i^0\right)^3 \left(r_j^0\right)^3}{\left(r_i^0\right)^6 + \left(r_j^0\right)^6}\right] \tag{4}$$

In the above equations, r_i^0 is the Lennard-Jones-9-6 parameter for atom i, r_j^0 is the Lennard-Jones-9-6 parameter for atom j, ε_i is the energy potential well depth for atom i, ε_j is the energy potential well depth for atom j, and r_{ij}^0 and ε_{ij} are combinations for a pair of atoms i and j. The two combination parameters r_{ij}^0 and ε_{ij} are used in the last two terms of the COMPASS model shown in equation (1). The term Lennard-Jones refers to the potential upon which these parameters are used. The Lennard-Jones-9-6 potential, which is the last term of the COMPASS` model, can and has been used by itself as a potential function. It is effective in modeling simple molecules and was originally used in the 1970s for the modeling of liquid argon[11].

Figure 2 shows snapshots of two molecular dynamics simulations of gaseous and liquid water. Figure 3 shows a snapshot of a molecular dynamics simulation of liquid DMAZ. Molecular dynamics can be used to compute the equilibrium and transport properties of a system of particles such as those in Figure 2[10,11]. This is done by expressing these properties as a function of the positions and momenta of the particles in the system.
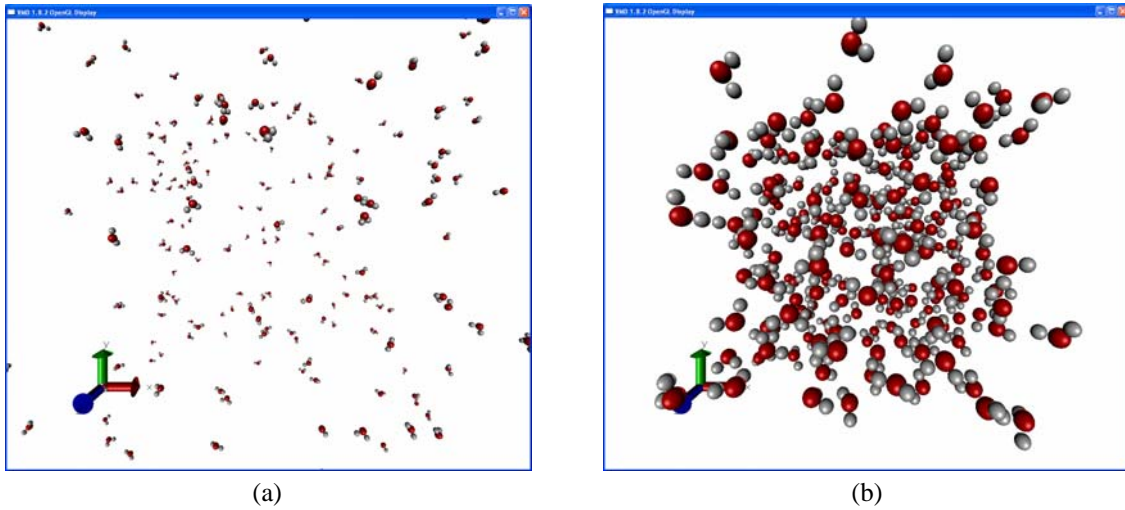
(a)   (b)

Figure 2. Molecular dynamics snapshots of (a) gaseous and (b) liquid water simulations
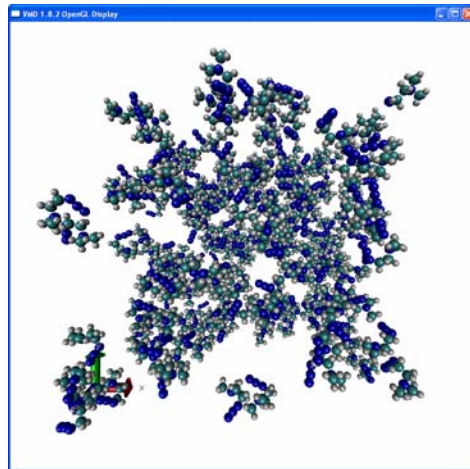

Figure 3. Molecular dynamics snapshot of liquid DMAZ simulation

The first observable that we define is kinetic energy per particle. For a system of point masses, the average kinetic energy per particle is defined using equation (5).

$$E_{kin} = \frac{1}{2N} \sum_{i=1}^{N} m_i \left(\vec{v}_i \cdot \vec{v}_i \right) \tag{5}$$

In the above equation, N is the number of particles in the system and m_i and v_i are the respective mass and velocity of particle i. In the case of polyatomic molecules, m_i is the mass of the molecule and v_i is the velocity of the center of mass of the molecule. From this definition of kinetic energy and making use of the principle of the equipartition of energy, the average translational temperature of the system particles (in three-dimensional space) can be defined as:

$$T_{trans} = \frac{1}{3Nk_B}\sum_{i=1}^{N} m_i(\vec{v}_i \cdot \vec{v}_i) = \frac{2}{3k_B}\left(\frac{1}{2N}\sum_{i=1}^{N} m_i(\vec{v}_i \cdot \vec{v}_i)\right) = \frac{2E_{kin}}{3k_B} \qquad (6)$$

where k_B is Boltzmann's constant. With the translational temperature defined, the pressure can then be easily defined as:

$$P = \frac{Nk_B T_{trans}}{V} + \frac{1}{3V}\sum_{i=1}^{N-1}\sum_{j=i+1}^{N}\sum_{\alpha=1}^{n}\sum_{\beta=1}^{n} \vec{f}_{ij}^{\,\alpha\beta} \cdot \vec{r}_{ij}^{\,\alpha\beta} \qquad (7)$$

where V is the volume of the computational space, $f_{ij}^{\alpha\beta}$ is the force vector of atom β of molecule j on atom α of molecule i, and $r_{ij}^{\alpha\beta}$ is the position vector from atom β of molecule j to atom α of molecule i. The first term is the ideal gas term while the second term is the configurational or "virial" term which becomes prominent at higher densities (farther away from the ideal gas assumption). Density is defined as:

$$\rho = \frac{N}{V}\sum_{i=1}^{N} m_i \qquad (8)$$

With these fundamental properties defined as a function of the positions and momenta of the particles, more complex properties can be defined. The first of these to be defined is enthalpy. We start by breaking up enthalpy into its two major components: enthalpy of formation and sensible enthalpy. Equation (9) shows the separation of enthalpy into its two components.

$$h(T,P) = \Delta h_f^0 + \Delta h \qquad (9)$$

In the above equation, Δh_f^0 is typically defined as the enthalpy of the particle at 298K and 1 atm. with respect to the arbitrary base in which the enthalpy of the elements that make up that particle is chosen to be zero in their natural states at the same temperature and pressure[12]. The second term, Δh, is known as the sensible enthalpy and is defined as the difference in enthalpy between any given state and the state in which the formation enthalpy is defined. In this research work, the total enthalpy is calculated using a combination of quantum mechanics or literature values for h_f^0 and the enthalpies calculated using molecular dynamics as follows:

$$h(T,P) = \Delta h_{f\_QM}^0 + \left[E_{kin}(T,P) + E_{pot}(T,P) + \frac{P}{\rho}\right] - \left[E_{kin}(T_0,P_0) + E_{pot}(T_0,P_0) + \frac{P_0}{\rho_0}\right] \qquad (10)$$

The first term on the right hand side of equation (10) is the enthalpy of formation either obtained from literature (if available) or from quantum mechanics. The second term, in brackets, is the enthalpy calculated by molecular dynamics at the desired temperature and pressure. The third term, in brackets, is the enthalpy calculated by molecular dynamics at 298K and 1 atm. The E_{pot} term is the potential energy calculated from the COMPASS energy potential. The E_{kin} term is the kinetic energy of the particles including translational and rotational energies. Vibrational energies are not modeled in this stage of work, but will be modeled in future work.

III.   Results

Work has been done in implementing the COMPASS model and running it for two very different compounds: water and DMAZ. The same procedure used for implementing the COMPASS model for these compounds can also be used for the creation of a modified model for use with other HEDM propellants. Ball and cylinder renderings of water and DMAZ are shown in Figure 4. These renderings are optimized geometries created with HyperChem, a

molecular modeling and simulation software from HyperCube, Inc[13]. In addition to the COMPASS model work, experimental work has been performed on DMAZ. Experimental measurements of density, viscosity, and thermal conductivity as a function of temperature have been performed. The results of these measurements will be used to validate and improve the COMPASS model.
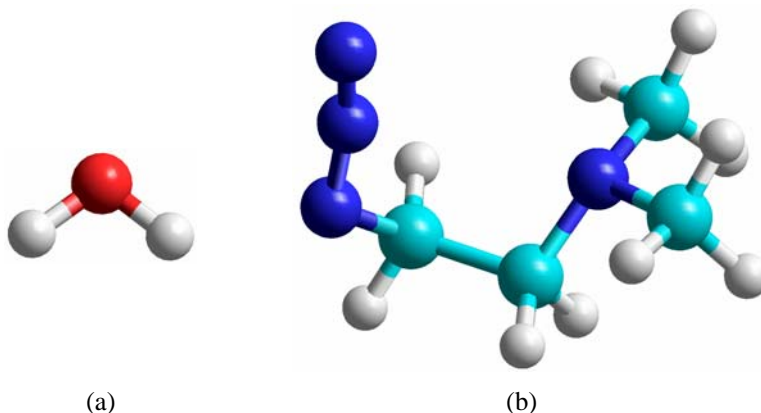

(a)   (b)

Figure 4. Ball and cylinder renderings of (a) water and (b) DMAZ. The cyan atoms are carbon atoms, the red atom is an oxygen atom, the blue atoms are nitrogen atoms, and the white atoms are hydrogen atoms.

A. Experimental Results

The following data in Tables 1, 2, and 3 below are experimental results from the testing of the density, shear viscosity, and thermal conductivity of DMAZ. The density results are compared with the computed values for DMAZ using the molecular dynamics technique to determine the accuracy of this method. Future work will include comparing the shear viscosity and thermal conductivity results with those computed using molecular dynamics. The density was measured using a high pressure pycnometer (Figure 5) and has an accuracy of ±0.2% with a reproducibility of ±0.05% (average of three data points)[14,15]. The shear viscosity was measured using a high pressure Cannon-Fenske viscometer (Figure 6) and has an accuracy of ±2.0% with a reproducibility of ±0.5% (average of three data points)[16,17]. The thermal conductivity was measured using a relative transient hot-wire method with a Pyrex capillary filled with mercury (Figure 7). This method has an accuracy of ±2.0% with a reproducibility of ±0.5% (average of five data points)[18].

Table 1. Density of DMAZ

P (bar)	T (K)	ρ (kg/m^3)
1.00	293.25	933.5
1.00	313.00	913.5
1.00	333.10	892.6
1.00	353.05	872.1
1.00	368.05	857.5
1.00	387.35	836.4
8.00	404.55	816.5
11.00	418.55	796.2
19.00	435.95	776.6

Figure 5. Cole-Farmer Pycnometer

Table 2. Shear Viscosity of DMAZ

P (bar)	T (K)	μ (cP)
1.00	293.25	0.721
1.00	313.00	0.564
1.00	333.10	0.456
1.00	353.05	0.379
1.00	368.05	0.335
1.00	387.35	0.284
1.00	406.05	0.255
8.00	406.35	0.249
15.00	421.55	0.235
19.00	438.95	0.209

Figure 6. Cannon-Fenske Routine Viscometer

Table 3. Thermal Conductivity of DMAZ

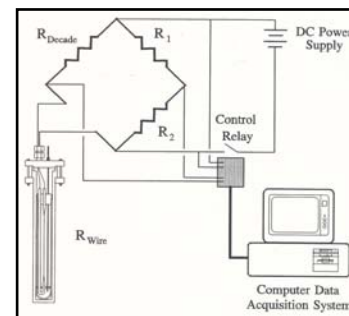| P (bar)	T (K)	λ (W/m-K)
1.00	297.40	0.133
1.00	324.90	0.125
1.00	349.30	0.118
8.00	374.30	0.112
11.00	398.50	0.107
19.00	425.30	0.101

Figure 7. Transient Hot-Wire Cell

B. Thermophysical Property Calculations

The following thermophysical data for water and DMAZ were calculated using the analysis technique described in Section II. The data is presented using real versus predicted plots with a diagonal line representing the experimental values.

Four types of molecular dynamics simulations were performed: two using water molecules and two using DMAZ molecules. For each type of molecule (water or DMAZ), two types of molecular dynamics simulations were performed. The first type was used to calculate enthalpy. This is done by holding constant the number of particles (N), the volume (V), and the temperature (T). The second type was used to calculate density. This is done by holding constant the number of particles (N), the pressure (P), and temperature (T). The molecular dynamics simulations which involved water consisted of 256 water molecules located in a cubic cell. The molecular dynamics simulation which involved DMAZ consisted of 108 DMAZ molecules located in a cubic cell. Pressure and temperature are held constant using techniques described in chapter 6 of reference 11. Periodic boundary conditions are used in all three dimensions. Periodic boundary conditions are a technique of surrounding the computational domain with exact replicas of the computational domain. This technique is useful in simulating thermodynamic properties that are based upon a continuum fluid[10]. Figure 8 is a schematic of this idea[11]. The central box is the computational domain and all the surrounding boxes are images of the central box.
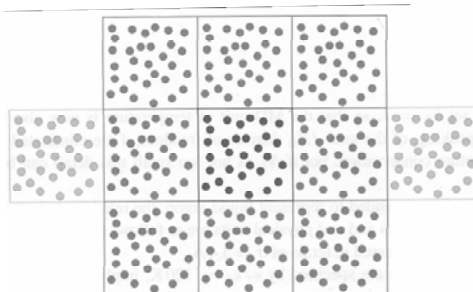

Figure 8. Schematic of periodic boundary conditions in two dimensions

The Lennard-Jones terms are modeled inside a cutoff distance of 7.5 Å for water and 13.0 Å for DMAZ. A long-range correction term is added to account for the potential not modeled outside this cutoff distance[10]. This cutoff distance is used to significantly reduce the computational time by not modeling the Lennard-Jones potential between two distant atoms whose potential is nearly zero. The long range Coulomb interactions are modeled using the Ewald summation technique[11,19]. This technique, used by most molecular dynamics simulations to model Coulomb interactions, is an efficient means of modeling these interactions without utilizing a cutoff distance. A cutoff distance is not used for modeling Coulomb interactions due to the fact that these interactions extend a much larger distance than do Lennard-Jones interactions. As seen in equation (1), Coulomb potential is proportional to r^{-1} as opposed to r^{-6} for Lennard-Jones interactions. The equations of motion for the system are modeled using a predictor-corrector method[11] with a time step $\Delta t = 0.83$ fs for water and $\Delta t = 0.48$ fs for DMAZ. The total duration of each simulation is 20,000 time steps including an equilibration run of 11,000 time steps. The equilibration run is performed in order to allow the molecules, which are initially placed in a cubic lattice, to move into a random configuration. Each data point is an average of 9 block averages of 1,000 time steps each from time step 11,000 to time step 20,000.

1. Water

The average pressure calculated at the input density and temperature of water ($\rho = 997$ kg/m^3, T = 298 K) is 6.53 bar. This error is considered satisfactory[8,9] since the isothermal compressibility (k_T) of water is $4.589*10^{-5}$ / bar[20]. A deviation of 6.53 bar in pressure corresponds to only a 0.03% error in the density of liquid water at 298 K.

Figure 9 shows actual versus predicted plots of the sensible enthalpy and density of water. The average absolute deviation in sensible enthalpy for the nine data points is 104.3kJ/kg. This translates to an average percentage deviation, when converted to absolute enthalpy (gas phase $\Delta h_f^{298} = -13,400$ kJ/kg), of 0.74%. The average absolute deviation in density is 30.5 kg/m^3 or 5.89%. These errors are considered acceptable for use in the conceptual design of rocket engines. As expected, the molecular dynamics simulations are most accurate at predicting the enthalpy and density of water in its gaseous and low pressure liquid states. The accuracy decreases at elevated pressures and at points near the critical point of water ($T_c=647$ K, $\rho_c = 322$ kg/m^3, $P_c=22.06$ MPa[21]). The data is provided in Table 4.

Table 4. Density and Sensible Enthalpy Estimates for Water

		Density (kg/m^3)		h_{sens} (kJ/kg)	
T (K)	P (MPa)	MD	Exp^a	MD	Exp^a
298.3	0.65	1000.20	997.26	-2305.6	-2440.5
311.0	0.08	979.30	993.01	22.3	23.2
388.5	0.11	0.59	0.60	161.3	160.0
450.0	20.00	856.50	902.30	-1567.1	-1787.0
467.0	0.21	0.95	0.97	300.2	311.5
550.0	20.00	645.14	775.70	-1087.9	-1330.9
800.0	80.00	336.40	403.05	129.9	21.4
950.0	40.00	102.47	104.89	946.2	1061.2
1000.0	80.00	196.71	208.86	885.1	988.7

^{a} Experimental data are from IAPWS (reference 21).

(a)   (b)
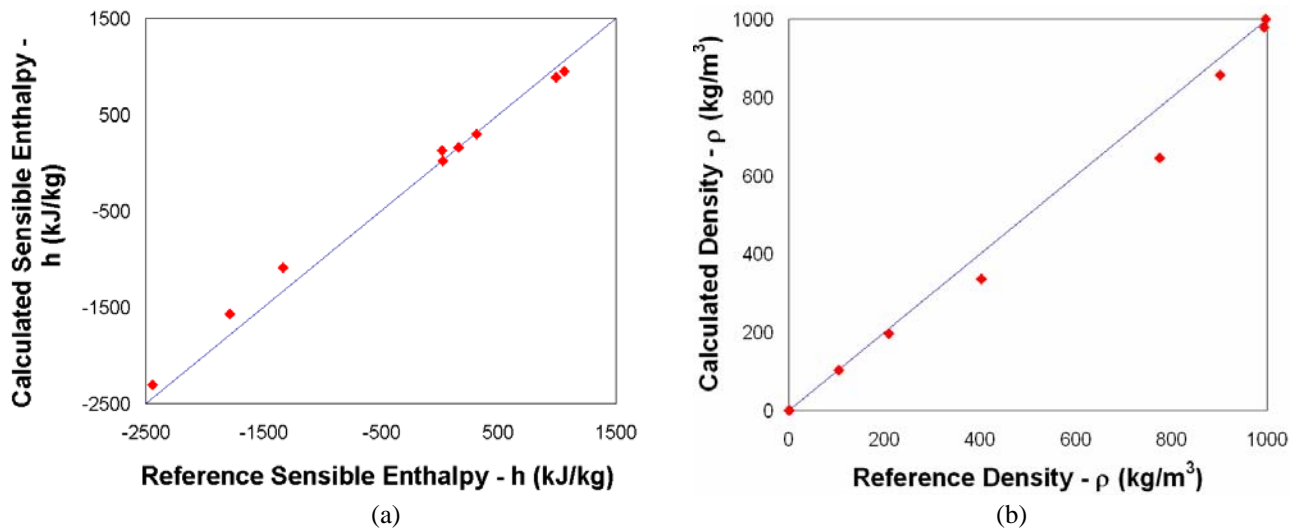
Figure 9. Actual vs. predicted plots of (a) sensible enthalpy and (b) density for water

American Institute of Aeronautics and Astronautics

2. DMAZ

Figure 10 is an actual versus predicted plot for the density of DMAZ. A small density range is used due to the lack of experimental density data for DMAZ. The actual values are taken from the experimental results provided in Table 1. The molecular dynamics model is less accurate at predicting the density of DMAZ than it is predicting the density of water. The average absolute deviation in density is 92.6 kg/m^3 or 10.58%. Improvements to the molecular dynamics model, including the incorporation of molecular vibrational effects, are expected to improve the accuracy. The data is provided in Table 5.

Table 5.   Density Estimates for DMAZ

T (K)	P (MPa)	Density (kg/m^3) MD	Exp^a
293.25	100	786.0	933.5
353.05	100	752.3	872.1
404.55	100	739.8	816.5
435.95	100	750.4	776.6

^{a} Experimental data from Table 1.

Table 6.   Sensible Enthalpy Estimates for DMAZ

T (K)	ρ (kg/m^3)	h_{sens} (kJ/kg) MD
404.1	331.2	48.8
493.1	331.2	88.8
655.0	331.2	162.8

Estimates of sensible enthalpy are provided in Table 6. McQuaid in reference 3 provides a Δh_f^{298} for condensed-phase DMAZ of 2,504 kJ/kg. With this data, one can begin to construct tables of density and total enthalpy (see equation (9)) as a function to temperature and pressure or temperature and density to be used in conceptual rocket engine design codes.
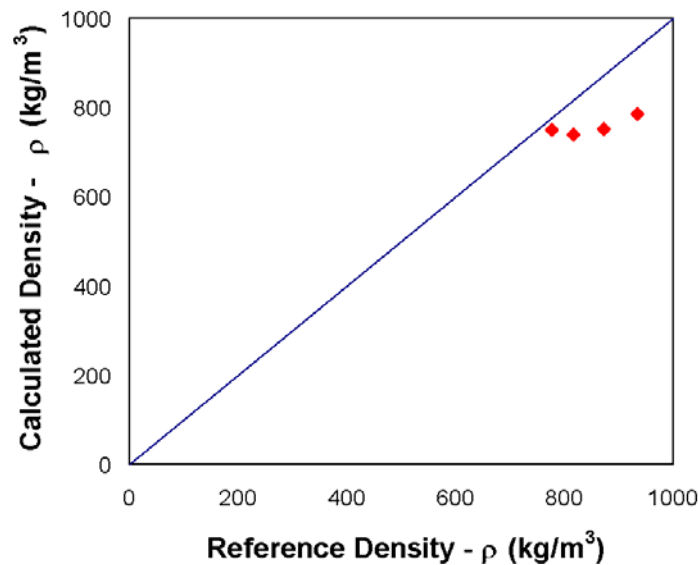

Figure 10.   Actual vs. predicted plot of density for DMAZ

C. Sensitivity Study

A sensitivity study of the changes in the thermophysical properties of a fuel and the effects of these changes on the propulsion system level outputs was performed. This study used the engine powerhead design code P-STAR with a liquid oxygen, liquid hydrogen staged-combustion cycle. The thermophysical properties of liquid hydrogen were altered to study the effects of its thermophysical properties on vacuum specific impulse, engine weight, and engine theoretical first unit (TFU) cost. The purpose of this study is to see which of the thermophysical properties need to be measured most accurately. Ideally the COMPASS model approach should be tailored to the accurate prediction of a particular thermophysical property which has the greatest influence on the engine level metrics at the cost of a somewhat less accurate prediction of other properties.

Figure 11 is a pareto plot of engine vacuum specific impulse as a function of hydrogen fuel enthalpy, entropy, and density. A pareto plot is used to determine the sensitivity of the response (I_{sp}, engine weight, TFU cost) to the various factors (enthalpy, entropy, and density). The horizontal axis indicates the contribution of the variation of a particular factor to the total variation of the response. The results shown in Figure 11 indicate that the variation in enthalpy contributes to more than 50% of the total variation in vacuum I_{sp}. The results also indicate that variation in entropy contributes nearly 50% of the total variation in vacuum I_{sp}. Fuel density has a very minimal effect on vacuum I_{sp}.
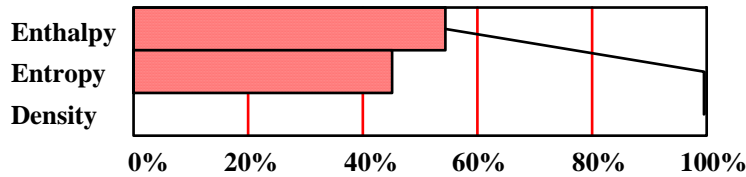
Figure 11. Pareto Plot of Vacuum I_{sp}

Figure 12 is a pareto plot of engine weight as a function of hydrogen fuel enthalpy, entropy, and density. The results indicate that engine weight is predominately affected by fuel density. Engine turbopumps are particularly affected by fuel density as density influences a variety of parameters such as pump efficiency and the number of pump stages. Entropy and enthalpy affect the engine weight to a much lesser extent.
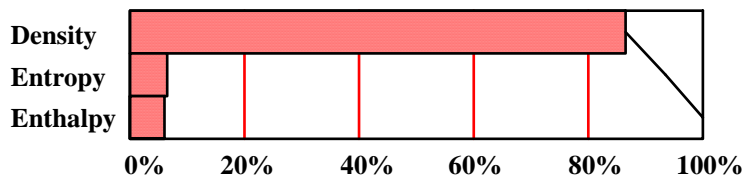
Figure 12. Pareto Plot of Engine Weight

Figure 13 is a pareto plot of engine TFU cost as a function of hydrogen fuel enthalpy, entropy, and density. The results follow the same trend as those seen in the engine weight pareto plot. These two pareto plot trends are similar because engine TFU is calculated using weight-based cost estimation relationships (CER).
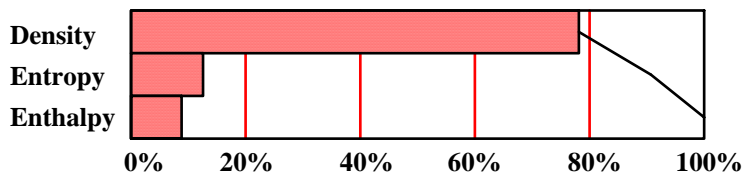
Figure 13. Pareto Plot of Engine TFU

These results do not show a clear need to tailor the COMPASS model to predict a particular thermophysical property more accurately than any other. A larger sensitivity study will be performed in the future incorporating both viscosity and thermal conductivity in addition to the three properties studied above. It is believed that the results of that study will show a relative importance of enthalpy, entropy, and density over viscosity and thermal conductivity for the engine level metrics analyzed. If that is the case, the COMPASS model can be tailored to model enthalpy, entropy, and density as accurately as possible while still modeling viscosity and thermal conductivity with reasonable accuracy.

IV. Future Work

Future work is required in several areas to make this technique more useful for engineers performing conceptual propulsion system designs utilizing new propellants. First, improvements need to be made to the molecular dynamics model to incorporate vibrational motion of the molecules. This motion is a factor for molecules at higher temperatures as the vibrational energy modes become excited. These high temperatures are common in rocket engines and thus the vibrational motion needs to be modeled in order to accurately predict the thermophysical properties over the entire temperature and pressure range.

Second, entropy needs to be calculated to model the equilibrium combustion in the engine combustor. As seen by the above sensitivity study, entropy plays an important role in the calculation of vacuum I_{sp} and needs to be modeled with accuracy. Entropy is calculated by making use of the partition function, Z. The partition function describes how the particles are divided up among different energy groups[22].

$$s = k_B \ln Z_{NVE} \tag{11}$$

$$Z_{NVE} = \sum_{i=1}^{N} \delta(E_i - E) \tag{12}$$

$$\delta(E_i - E) = \sqrt{(E_i - E)^2} \tag{13}$$

$$E = \sum_{i=1}^{N} E_i \tag{14}$$

In the above equations, Z_{NVE} is the partition function for simulations with the number of particles (N), the volume (V), and the total energy (E) held constant. E_i is the total energy of particle i. E is the average total energy per particle.

Third, shear viscosity and thermal conductivity need to be calculated to be able to fully incorporate this molecular dynamics technique in the powerhead design of rocket engines. Viscosity and thermal conductivity are needed for pump, turbine, and heat exchanger analyses. Shear viscosity (or absolute viscosity) and thermal conductivity are two properties known as transport properties. Unlike density, enthalpy, and entropy which are measured at equilibrium, viscosity and thermal conductivity are time-dependent properties which are defined differently from the equilibrium properties. In order to define these two properties in molecular dynamics, we need to introduce the idea of an autocorrelation function. An autocorrelation function measures the correlation between some parameter such as velocity, pressure, or heat flux of a particle at two different points in time[10,11]. Using the integrated autocorrelation function of the pressure tensor, the Green-Kubo form of shear viscosity is shown below.

$$\mu = \frac{V}{3k_B T} \int_0^\infty \left\langle P^{xy}(t)P^{xy}(0) + P^{yz}(t)P^{yz}(0) + P^{xz}(t)P^{xz}(0) \right\rangle dt \tag{15}$$

$$P^{xy} = \frac{1}{V}\left(\sum_{i=1}^{N} m_i v_i^x v_i^y + \frac{1}{2}\sum_{i=1}^{N-1} \sum_{j=i+1}^{N} r_{ij}^x f_{ij}^y \right) \tag{16}$$

In the above equations $\langle \ldots \rangle$ denotes the ensemble average, v_i^x is the x-component of the velocity vector of particle i, v_i^y is the y-component of the velocity vector of particle i, r_{ij}^x is the x-component of the position vector from particle j to particle i, and f_{ij}^y is the y-component of the force vector of particle j on particle i. Similarly, thermal conductivity is defined using the integrated heat flux autocorrelation function:

$$\lambda = \frac{V}{3k_B T^2} \int_0^\infty \left\langle \bar{J}(t) \cdot \bar{J}(0) \right\rangle dt \tag{17}$$

$$\bar{J} = \frac{1}{V}\left(\sum_{i=1}^{N}\hat{e}_i\bar{v}_i + \frac{1}{2}\sum_{i=1}^{N}\sum_{j=1(j\neq i)}^{N}\bar{r}_{ij}\left(\bar{f}_{ij}\cdot\bar{v}_j\right)\right)$$ (18)

$$\hat{e}_i = \frac{1}{2}m_i\left(\bar{v}_i\cdot\bar{v}_i\right) + \frac{1}{2}\sum_{i=1}^{N}\sum_{j=1(j\neq i)}^{N}E_{pot}\left(\bar{r}_{ij}\right) - \frac{1}{N}\sum_{j=1}^{N}e_j$$ (19)

In the above equations, $\hat{e}_i$ is the instantaneous excess energy of particle i, v_i is the velocity vector of particle i, E_{pot} is the energy potential of particle i due to particle j, r_{ij} is the position vector from particle j to particle i, and e_j is the energy of particle j.

The fourth area in which future work is needed is the experimental measurement of the specific heat of DMAZ as a function of temperature using a differential scanning calorimeter. This information can be used to determine the enthalpy and entropy change of DMAZ as a function of temperature. This experimental data can then be compared against the molecular dynamics predictions of these properties.

The fifth area of future work is the detailed study of the predictive accuracy of the COMPASS model for higher energy compounds such as DMAZ (Figure 4c), quadricyclane, cubane (Figure 14), and other HEDM propellants. It is believed that this model will not adequately predict the necessary thermophysical properties for these types of molecules and will thus need to be modified. This modification may simply be new sets of coefficients for these types of molecules or may require more substantial additions of terms to the COMPASS potential equation. It is believed that HEDM propellants are more difficult to model using the COMPASS force field, because their particular molecular structure lends to a stronger interaction between internal coordinates. This stronger interaction may require the use of a different set of cross-coupling terms to more accurately model these types of molecules.
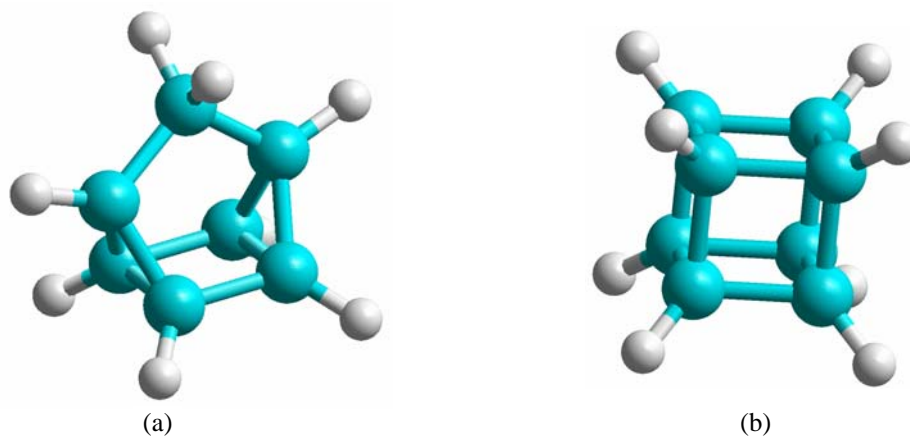

(a)   (b)

Figure 14. Ball and cylinder renderings of (a) quadricyclane (C_7H_8) and (b) cubane (C_8H_8). The cyan atoms are carbon atoms and the white atoms are hydrogen atoms.

The sixth and final area of future work is the prediction and compilation of all the necessary thermophysical properties for a variety of potential new propellants. These properties will then be incorporated in a powerhead design tool and then used in the conceptual design of a liquid rocket engine as part of an overall conceptual vehicle design. This will allow one to quantify the benefits of using these new propellants to the overall vehicle and its corresponding space or launch architecture.

Acknowledgments

Georgia Institute of Technology. The authors would also like to thank Dr. Tongfan Sun for his work on the measurement of the physical properties of DMAZ.

References

[1] Wucherer, E.J. and A. Wilson. "Chemical, Physical and Hazards Properties of Quadricyclane." U.S. Air Force Research Laboratory, Edwards Air Force Base, California. PL-TR-97-3053, March 1998.

[2] Tishkoff, J.M. and M.R. Berman. "Air Force Basic Research in Propellants and Combustion." U.S. Air Force Office of Scientific Research, Arlington, Virginia. AIAA Paper 2002-0901, January 2002.

[3] McQuaid, M.J. "Computational Characterization of 2-Azidocycloalkanamines – Notional Variations on the Hypergol 2-Azido-N,N-Dimethylethanamine (DMAZ)." U.S. Army Research Lab. JANNAF 30th Propellant Development and Chracterization Subcommittee Meeting, pp. 45-57, March 2002.

[4] McQuaid, M.J. "Structure of Secondary 2-Azidoethanamines: A Hypergolic Fuel vs. a Nonhypergolic Fuel." U.S. Army Research Laboratory, Aberdeen Proving Ground, MD. ARL-TR-3176, April 2004.

[5] Bai, S.D., Dumbacher, P., and J.W. Cole. "Development of Advanced Hydrocarbon Fuels at Marshall Space Flight Center." NASA/TP – 2002-211729, May 2002.

[6] Levine, I.N. *Quantum Chemistry, Fifth Edition*, Prentice Hall. Upper Saddle River, New Jersey, 2000.

[7] Pang, T. *An Introduction to Computational Physics,* Cambridge University Press. Cambridge, UK , 1997.

[8] Sun, H., "COMPASS: An ab Initio Force-Field Optimized for Condensed-Phase Applications – Overview with Details on Alkane and Benzene Compounds," *Journal of Physical Chemistry B*, 102: 7338-7364, 1998.

[9] McQuaid, M.J., H. Sun, and D. Rigby, "Development and Validation of COMPASS Force Field Parameters for Molecules with Aliphatic Azide Chains," *Journal of Computational Chemistry*, 25: 61-71, 2004.

[10] Frenkel, D. and B. Smit, *Understanding Molecular Simulation, From Algorithms to Applications*, Academic Press. San Diego, California, 1996.

[11] Rapaport, D.C., *The Art of Molecular Dynamics Simulation, Second Edition*, Cambridge University Press. Cambridge, United Kingdom, 2004.

[12] Van Wylen, G., R. Sonntag, and C. Borgnakke, *Fundamentals of Classical Thermodynamics*, John Wiley & Sons, Inc. New York, New York, 1994.

[13] "HyperChem Release 7 for Windows, Getting Started," HyperChem Manual, Publication HC70-00-01-00, HyperCube, Inc. January 2002.

[14] "Standard Test Method for Density and Relative Density of Liquids by Bingham Pycnometer," ASTM Standard D 1217-93, ASTM International, West Conshohocken, Pennsylvania, 2003.

[15] "Standard Test Method for Density and Relative Density of Viscous Materials by Lipkin Bicapillary Pycnometer," ASTM Standard D 1481-02, ASTM International, West Conshohocken, Pennsylvania, 2002.

[16] "Standard Test Method for Kinematic Viscosity of Transparent and Opaque Liquids and the Calculation of Dynamic Viscosity," ASTM Standard D 445-04, ASTM International, West Conshohocken, Pennsylvania, 2004.

[17] "Standard Specifications and Operating Instructions for Glass Capillary Kinematic Viscometers," ASTM Standard D 446-04, ASTM International, West Conshohocken, Pennsylvania, 2004.

[18] Bleazard, J.G., "The Thermal Conductivity of Aqueous Electrolyte Solutions and Polar Liquids," Ph.D. Dissertation, Georgia Institute of Technology. Atlanta, Georgia, 1995.

[19] Sadus, R.J., *Molecular Simulation of Fluids: Theory, Algorithms and Object-Orientation*, Elsevier Science B.V., Amsterdam, The Netherlands, 1999.

[20] London South Bank University. "Water Data (supplementary)." Online. Internet. 2 July 2005. Available: http://www.lsbu.ac.uk/water/data1.html.

[21] International Association for the Properties of Water and Steam (IAPWS), Online. Internet 5 May 2005. Available: http://www.cheresources.com/iapwsif97.shtml.

[22] Vincenti, W.G. and C.H. Kruger, Jr., *Introduction to Physical Gas Dynamics*, John Wiley & Sons. New York, New York, 1965.